Hydroxyapatite Augmentation for Bone Atrophy in Total Ankle Replacement in Rheumatoid Arthritis

Kenrin Shi, MD, PhD,[1] Kenji Hayashida, MD, PhD,[2] Jun Hashimoto, MD, PhD,[3] Kazuomi Sugamoto, MD, PhD,[4] Hideo Kawai, MD, PhD,[5] and Hideki Yoshikawa, MD, PhD[6]

Although total ankle replacement is routinely used for rheumatoid arthritis of the ankle, it has been hampered by early implant failures such as loosening and subsidence of the tibial component due to poor bone quality. To prevent this complication, total ankle replacement augmented by a specially designed hydroxyapatite coating was used in 14 patients (16 feet). Patients were reviewed after an average follow-up of 23.1 months, and the mean clinical rating scale significantly improved from 30.7/100 points preoperatively to 65.9/100 at final follow-up, especially with respect to pain relief. Radiographs taken immediately postoperatively and at final follow-up were analyzed for the position and sinking of the tibial component. The position was evaluated by measurement of the alpha and beta angles, formed by the tibial long axis and tibial component on anteroposterior and lateral radiographs, respectively. The mean alpha and beta angles were 87.4° and 79.3° postoperatively and 87.7° and 81.0° at final follow-up, respectively. No significant change was noted in either angle between the immediate postoperative views and at final follow-up, and no significant subsidence was noted. Radiographs were also assessed for the presence of a lucent zone: 1 case demonstrated a clear zone between hydroxyapatite and bone, 9 cases between hydroxyapatite and the tibial component, and 6 cases between the tibial component and bone. These results suggest that hydroxyapatite helps to secure implant fixation firmly to the bone, making it a useful augmentation for tibial bone atrophy in total ankle replacement for rheumatoid arthritis. (The Journal of Foot & Ankle Surgery 45(5):308–315, 2006)

Key words: rheumatoid arthritis, total ankle replacement, hydroxyapatite

Arthritic involvement of ankle joint is often observed in patients with rheumatoid arthritis (RA) in middle to late stages of the disease. Miehlke et al (1) stated that 52% of 300 patients had presented ankle and subtalar involvement with an average duration of 9.5 years. Because the ankle joint is a weight-bearing joint like the hip and knee, ankle destruction severely impairs standing and walking ability and disturbs a patient's quality of life. Arthrodesis had long been almost the only surgical treatment for this condition before the introduction of total ankle replacement (TAR). However, high nondelayed or delayed union rates after arthrodesis exist, possibly because of poor immunologic and metabolic conditions in patients with RA treated with steroid-type or antimetabolite-type medications (2).

TAR was first introduced in the early 1970s as an alternative to ankle arthrodesis, but high complication rates of early prosthesis designs such as severe osteolysis, component loosening, impingement, infection, and soft tissue breakdown were reported (3). These first-generation TAR prostheses often consisted of 2 components, tibial and talar, with a highly constrained design, and were thought to result in early failure because of the increased force between the bone and implant (4, 5).

The second-generation TAR with a less constrained component design was introduced in the 1980s; some can be fixated without cement and some possess a mobile-bearing (three-component) design. Kofoed and Sorensen reported no significant difference in clinical outcomes in patients with RA versus osteoarthritis (OA) with the use of the cemented Scandinavian Total Ankle Replacement (STAR) prosthesis, one of the second-generation TAR implants (6). These recent successful results have encouraged surgeons to perform TAR instead of arthrodesis, even in RA.

Address correspondence to: Kenrin Shi, MD, 4-8-1 Hoshigaoka, Hirakata, Osaka, 573-8511, Japan. E-mail: kenrin1968@yahoo.co.jp

[1]Staff doctor, Department of Orthopedics, Hoshigaoka Koseinenkin Hospital, Osaka, Japan.

[2]Director, Department of Orthopedics, Hoshigaoka Koseinenkin Hospital, Osaka, Japan.

[3]Assistant professor, Department of Orthopaedic Surgery, Osaka University Medical School, Osaka, Japan.

[4]Associate professor, Department of Orthopaedic Surgery, Osaka University Medical School, Osaka, Japan.

[5]Vice president, Department of Orthopedics, Hoshigaoka Koseinenkin Hospital, Osaka, Japan.

[6]Professor and chairman, Department of Orthopaedic Surgery, Osaka University Medical School, Osaka, Japan.

1067-2516/06/4505-0001$32.00/0
doi:10.1053/j.jfas.2006.06.001

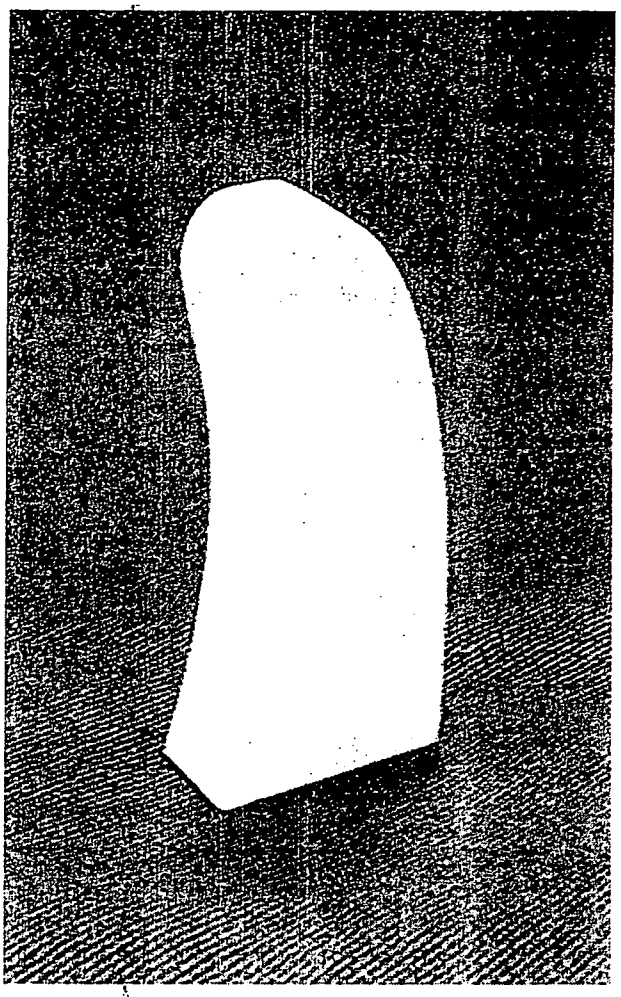

FIGURE 1 HA used in this study for tibial augmentation.

Although TAR has been performed in patients with RA increasingly in this decade, and favorable clinical outcomes with significant pain relief have been achieved, early implant failure such as loosening and subsidence of the implants is still a problem, often because of poor bone quality of the implanted site (4). As an attempt to solve this problem, especially in fixation of the tibial component, we used a specifically designed hydroxyapatite (HA) to augment the tibial bone atrophy in conjunction with TAR for rheumatoid ankles. The purpose of this article is to report the short-term outcomes and radiographic findings of this procedure.

Materials and Methods

HA (Boneceram; Olympus Biomaterial Corp., Tokyo, Japan) was designed and formed such that it could be inserted into the tibia easily, but would fit within the inner cortex of the distal tibia (Fig 1). The sizes of the HA component were determined according to previously obtained data of the transverse and sagittal diameter of the inner cortex of the distal tibia on anteroposterior (AP) and lateral radiographs of patients with RA (K. S., unpublished data, 1999).

TABLE 1 Clinical rating scale

Pain	
None	40
Mild	30
Moderate	20
Severe	10
Disabled	0
Function	
Walking distance	
Unlimited	20
2 km	15
0.5–2 km	10
Indoors only	5
Unable to walk	0
Limping	
None	4
Moderate	2
Unable to walk	0
Stairs (up)	
Normally	4
Needs banister	2
Unable	0
Stairs (down)	
Normally	4
Needs banister	2
Unable	0
Standing on operated leg	
Normally	4
Needs support	2
Unable	0
Sitting Japanese style	
Normally	4
Easy posture	2
Unable	0
Dorsiflexion	
11°–	10
6°–10°	7
1°–5°	4
0°	0
Plantarflexion	
36°–	10
21°–35°	7
6°–20°	4
5°	0

Outcomes were evaluated clinically and radiographically. Clinically, each ankle was scored according to a rating scale created by Takakura et al (7), which includes an assessment of pain relief as well as functional improvement such as walking ability, the ability to climb stairs, and range of motion (Table 1). The physical examination and patient interview were conducted by each surgeon preoperatively, but by the first author (K. S.) at final follow-up. Scores rated before the surgery and at the last follow-up were compared

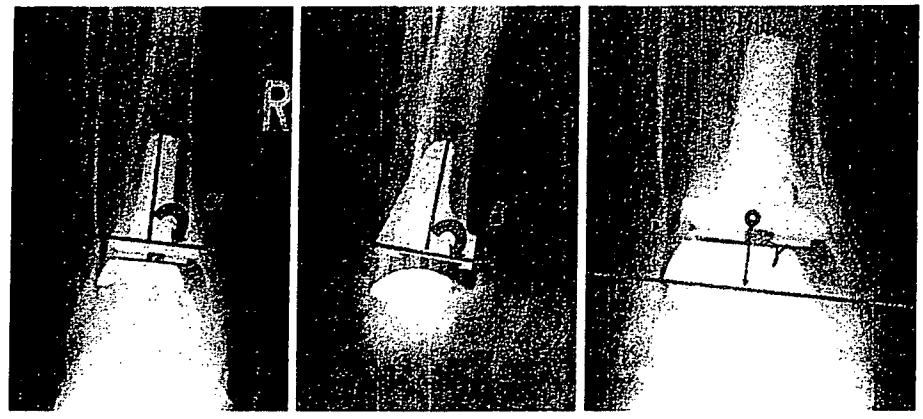

FIGURE 2 Radiographic evaluation of placement and subsidence of the tibial component. (*A*) Alpha angle. (*B*) Beta angle. (*C*) Gamma length.

and statistically examined by Wilcoxon signed-rank test. *P* values $<.05$ were considered to be significant.

AP and lateral radiographs taken immediately postoperatively and at final follow-up were compared with respect to the placement and migration of the tibial component. Placement was assessed with 2 angles: 1) the alpha angle, formed by the long axis of the tibia and the transverse line of the tibial component on the AP radiograph (Fig 2, A); and 2) the beta angle, formed by the long axis of the tibia and the sagittal line of the tibial component on lateral radiographs (Fig 2, B). Subsidence was evaluated by the following measurement on AP radiographs. First, a baseline that crossed the most prominent part of medial malleolus was determined perpendicular to the tibial long axis. Then, the length from the center of the tibial component to the baseline was measured and defined as the gamma length (Fig 2, C). Finally, the clear zone, determined as the radiolucent zone around the implant with a width ≥ 1 mm, was also assessed on AP radiographs as an indication of early loosening, either between the HA and the bone, HA and the tibial component, or the tibial component and bone. These radiographic data were obtained solely by the first author (K. S.), independent from the operating surgeons. Data obtained from radiographs taken immediately postoperatively and at the last follow-up were compared and statistically examined by use of Wilcoxon signed-rank test, with *P* values $<.05$ recognized as significant.

Surgical Technique

All procedures were performed through an anterior approach. After bone resection from the distal tibia, retrograde intramedullary rasping was performed to allow insertion of the HA. Then the HA was inserted into the tibia from the inferior aspect of the tibia, with its apex directed proximally and anteriorly. A TNK implant (Japan Medical Materials Corporation, Osaka, Japan) was used in all cases except 1, in which a FINE (Nakashima Medical, Okayama, Japan) was used. The TNK uses ceramic components with polyethylene on a tibial-bearing surface (8), whereas the FINE consists of metal tibial and talar components with a polyethylene mobile bearing between the components (9). All implants were fixated with bone cement. Concurrent subtalar joint arthrodesis was performed in 11 ankles that demonstrated subtalar deformity, erosion, and/or instability. All procedures were performed by one of 3 senior authors (K. H., J. H., K. Su.).

Ankles without subtalar arthrodesis were immobilized in a soft splint for 3 weeks, and then range-of-motion exercises and full weight bearing were started. Ankles with subtalar arthrodesis were immobilized in a short leg cast for 4 to 6 weeks, and full weight bearing was permitted 10 weeks postoperatively.

Results

Sixteen ankles (14 patients) were studied with a mean follow-up period of 23.1 months (range, 7–73 months). Two patients were men and 12 were women. Two patients underwent surgery on bilateral ankles separately. The mean patient age was 61.4 years (range, 48–74 years).

Clinical rating scale scores improved from 30.7 points (range, 14–42) preoperatively to 65.9 points (range, 27–86) at final follow-up (Fig 3).

Radiographic measurements are shown in Table 2. The mean alpha angle was 87.4° (range, 82.5–95°) postoperatively and 87.7° (range, 81.5–97°) at final follow-up. The mean beta angle was 79.3° (range, 72–89°) and 81.0° (range, 49–102°), respectively. The change in each angle from immediately postoperatively to the time of final follow-up was not found to be significant. The mean gamma length was 11.8 mm (range, 7–19 mm) postoperatively and 12.0 mm (range, 7.5–20 mm) at final follow-up, and no significant difference was found between these values. The

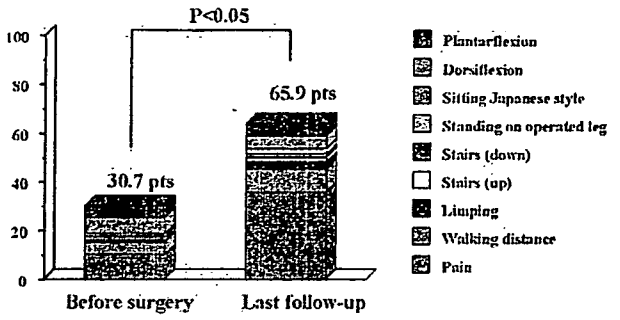

FIGURE 3 Clinical rating scale scores before surgery and at last follow-up.

TABLE 2 Results of radiographic evaluation of tibial component

	Postoperative	Last Follow-Up	*P* Value
Alpha angle	87.4	87.7	NS
Beta angle	79.3	81	NS
Gamma length (mm)	11.8	12	NS

Abbreviation: NS, not significant.

mean amount of sinking, defined as the increase of gamma length, was 0.2 mm.

One ankle demonstrated a clear zone between the HA and bone, 9 exhibited a clear zone between HA and the tibial component (Fig 4), and 6 demonstrated a clear zone between the tibial component and bone. Two ankles demonstrated early loosening, recognized as implant migration on radiographs. One of these underwent revision 6 months after the primary surgery (Fig 5). No clear zone was observed between HA and bone in either of these 2 cases. In the ankle that underwent revision, firm fixation between HA and bone was confirmed during the revision surgery.

Discussion

The first-generation TAR, introduced in the 1970s, resulted in high complication rates and early failures because of increased force between the bone and implant due to their highly constrained design (3–5). The second-generation TAR, introduced in the 1980s, has a less constrained design and, so far, has been used with favorable clinical results (6). Anderson et al (10) also reported a similar revision and loosening rate in patients with RA and OA after uncemented STAR prosthesis, with an estimated 5-year survival rate of 70%, with revision as the end point. Another second-generation TAR was reported to present a 5-year survival rate of 54%, in a study of mostly relatively young patients with posttraumatic or primary OA (11).

However, even in such prostheses with advanced designs,

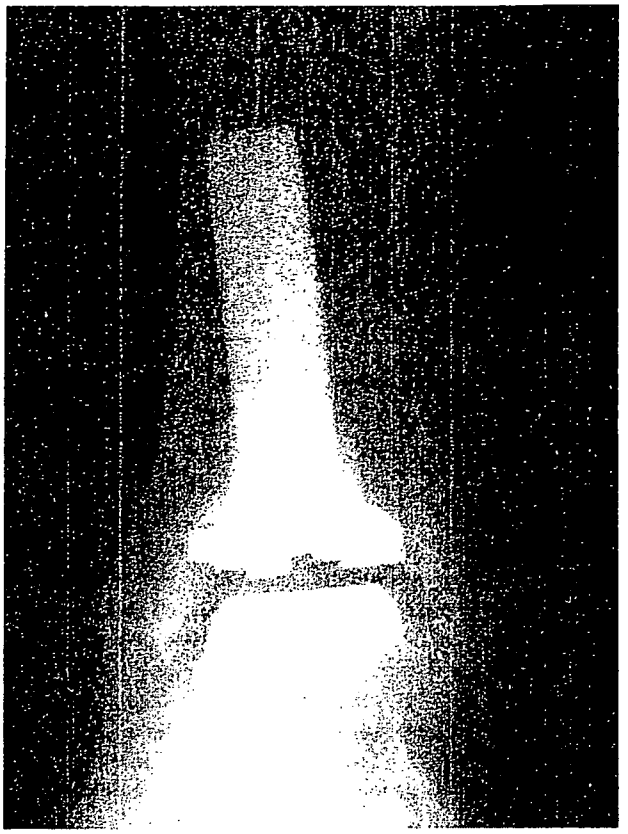

FIGURE 4 AP radiograph demonstrating a clear zone between HA and the tibial component. In this case, a clear zone between HA and the tibial component was obvious, whereas no clear zone was recognized between HA and bone or between bone and the tibial component.

arthritic involvement and deformity in hindfoot and other major lower extremity joints can lead to early failure of the ankle prosthesis in patients with RA (12). Kofoed and Sorensen reported that a progression of hindfoot valgus deformity resulted in failure of TAR in patients with RA (6). A radiographic evaluation of the ankle and subtalar joint of patients with RA has also shown that subtalar pathology precedes changes in the ankle joint in the natural course of RA (13). For this reason, the authors performed corrective arthrodesis of subtalar joint not only in patients with an existing subtalar deformity, but also in those demonstrating subtalar erosion and/or instability that would be expected to cause valgus deformity or pain.

Another issue contributing to early failure in TAR in RA is implant migration due to poor bone quality. Of the 12 revisions in the report by Anderson et al (10), the reason for revision was loosening of the tibial component in 2 patients, the talar component in 2 patients, and both components in 3 patients. Carlsson et al (14) also reported a similar migration pattern of tibial and talar components of the STAR prosthe-

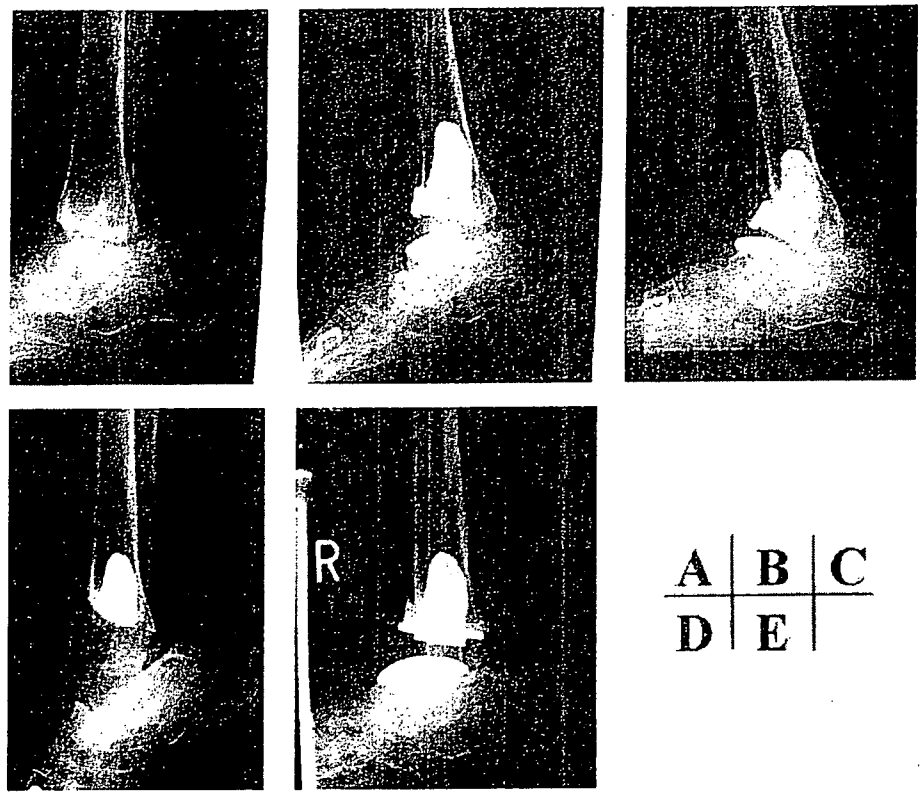

FIGURE 5 A case of a 64 year-old woman who demonstrated early loosening that necessitated a revision surgery 5 months after the initial surgery. However, no clear zone was observed between HA and bone on radiographs, and firm fixation between HA and the implanted site was confirmed during the revision surgery. (*A*) Before surgery. (*B*) After the initial surgery. (*C*) Loosening of the tibial component was noted. (*D*) Firm bonding of HA with the implanted site bone was noted after removal of the tibial component. (*E*) After the revision surgery.

sis after 3 to 5 years of follow-up. On the other hand, Su et al (15) reported that 3 of 26 ankles presented subsidence of the tibial component after an uncemented TAR. In this study, HA was only used for augmentation of tibial bone atrophy, partly because subtalar arthrodesis was performed in many cases, preventing the bulk augmentation of the talus in those cases.

Over the last 2 decades, HA has been used to augment bone loss more in facial and dental surgery than orthopedic surgery because of concern about its ability to withstand weight-bearing forces (16, 17). However, clinical reports of HA used for spine surgery (18) and revision total hip arthroplasty (19) have encouraged its use in lower extremity surgery. As for the HA used in this study, Itokazu and Matsunaga (20) reported the use of this material as a graft in bone defect in the treatment of tibial plateau fractures. Koshino et al (21) used a wedge-shaped block of Boneceram in a medial open-wedge proximal tibial ostotomy for knee OA without collapse or subsidence.

The results of the current study show that the position of the tibial implant was secured without migration in most cases, and this compound could be helpful in securing the initial placement of the implant. Neither breakage nor collapse of HA was observed. In addition, firm bonding with the bone was demonstrated radiographically in most cases and intraoperatively in 1 case during the revision surgery. Although histological examination was not performed in this case, a previous study has shown incorporation into the surrounding bone (20). Therefore, this material provides an option for augmentation of tibial bone atrophy in TAR in patients with RA.

HA is now also used in several types of cementless TAR as a coating material over metal implants similar to other joint prostheses, to promote firm bonding between the bone and implant. Bonnin et al reported decreased radiolucency with the use of the Salto prosthesis (Tornier SA, Saint Ismier, France) with HA coating (22). Kofoed reported a longer survival rate of cementless HA-coated STAR prosthesis (Waldemar Link, Hamburg, Germany) as compared with a cemented implant at a mean 12 years postoperatively (23). Moreover, a double-coated prosthesis, coated with 300 μm plus 25 μm thickness of HA, has recently been introduced (24). Its radiostereometric analysis demonstrated initial migration of both tibial and talar components at 6 weeks without progression or bone resorption, and there was no difference in these results between patients with RA and OA (14). In addition to bulk augmentation as it was used in this study, HA may also be a promising agent for implant fixation in TAR.

The results of this study do demonstrate one major concern: the high frequency of radiolucency. More than half of the ankles studied demonstrated a clear zone between HA and

the tibial component on radiographs at the final follow-up. Two ankles resulted in radiographic loosening recognized as implant migration, one of which required revision. Although firm bonding between HA and bone was recognized, a certain limitation remains, in that cement fixation between HA and the implant was unsatisfactory. Perhaps the amount of pressurization during solidification of bone cement may not have been adequate.

In conclusion, the HA presented in this study provides an option for augmentation of tibial bone atrophy in TAR for patients with RA, because it bonded firmly to bone at the implantion site. Migration or subsidence of the tibial implant was not observed in most cases. Methods for firm fixation of implants with HA should be developed, and bonding of HA with bone should be scrutinized over a longer-term follow-up.

References

1. Miehlke W, Gschwend N, Rippstein P, Simmen BR. Compression arthrodesis of the rheumatoid ankle and hindfoot. Clin Orthop 340: 75–86, 1997.
2. Nassar J, Cracchiolo A 3rd. Complications in surgery of the foot and ankle in patients with rheumatoid arthritis. Clin Orthop Relat Res Oct:140–152, 2001.
3. Bolton-Maggs BG, Sudlow RA, Freeman MAR. Total ankle arthroplasty. A long-term review of the London Hospital experience. J Bone Joint Surg Br 67:785–790, 1985.
4. Conti SF, Wong YS. Complications of total ankle replacement. Clin Orthop 391:105–114, 2001.
5. Easley MD, Vertullo CJ, Urban WC, Nunley JA. Perspectives on modern orthopaedics. Total ankle arthroplasty. J Am Acad Orthop Surg 10:157–167, 2002.
6. Kofoed H, Sorensen TS. Ankle arthroplasty for rheumatoid arthritis and osteoarthritis. Prospective long term study of cemented replacement. J Bone Joint Surg Br 80:328–332, 1988.
7. Takakura Y, Tanaka Y, Sugimoto K, Tamai S, Masuhara K. Ankle arthroplasty. A comparative study of cemented metal and uncemented ceramic prostheses. Clin Orhop 252:209–216, 1990.
8. Takakura Y, Tanaka Y, Kumai T, Sugimoto K, Ohgushi H. Ankle arthroplasty using three generations of metal and ceramic prostheses. Clin Orhop 424:130–136, 2004.
9. Nakashima Medical. Available at: http://www.nakashima.co.jp/Medical/product/ashi.html. Accessed December 20, 2005.
10. Anderson T, Montgomery F, Carlsson A. Uncemented STAR total ankle prostheses. Three to eight-year follow-up of fifty-one consecutive ankles. J Bone Joint Surg Am 85:1321–1329, 2003.
11. Spirt AA, Assal M, Hansen ST Jr. Complications and failure after total ankle arthroplasty. J Bone Joint Surg Am 86:1172–1178, 2004.
12. Felix NA, Kitaoka HB. Ankle arthrodesis in patients with rheumatoid arthritis. Clin Orthop 349:43–47, 1998.
13. Belt EA, Kaarela K, Maenpaa H, Kauppi MJ, Lehtinen JT, Lehto MU. Relationship of ankle joint involvement with subtalar destruction in patients with rheumatoid arthritis. A 20-year follow-up study. Joint Bone Spine 68:154–157, 2001.
14. Carlsson A, Markusson P, Sundberg M. Radiostereometric analysis of the double-coated STAR total ankle prosthesis: a 3–5 year follow-up of 5 cases with rheumatoid arthritis and 5 cases with osteoarthrotis. Acta Orthop 76:573–579, 2005.
15. Su EP, Kahn B, Figgie MP. Total ankle replacement in patients with rheumatoid arthritis. Clin Orthop 424:32–38, 2004.
16. Jarcho M. Retrospective analysis of hydroxyapatite development for oral implant applications. Dent Clin North Am 36:19–26, 1992.
17. Zeltser C, Masella R, Cholewa J, Mercier P. Surgical and prosthodontic residual ridge reconstruction with hydroxyapatite. J Prosthet Dent 62:441–448, 1989.
18. Spivak JM, Hasharoni A. Use of hydroxyapatite in spine surgery. Eur Spine J 10:S197–S204, 2001.
19. Oonishi H, Iwaki Y, Kin N, Kushitani S, Murata N, Wakitani S, Imoto K. Hydroxyapatite in revision of total hip replacements with massive acetabular defects: 4- to 10-year clinical results. J Bone Joint Surg Br 79:87–92, 1997.
20. Itokazu M, Matsunaga T. Arthroscopic restoration of depressed tibial plateau fractures using bone and hydroxyapatite grafts. Arthroscopy 9:103–108, 1993.
21. Koshino T, Murase T, Saito T. Medial opening-wedge high tibial ostetomy with use of porous hydroxyapatite to treat medial compartment osteoarthritis of the knee. J Bone Joint Surg Am 85:78–83, 2003.
22. Bonnin M, Judet T, Colombier JA, Buscayret F, Graveleau N, Piriou P. Midterm results of the Salto Total Ankle Prosthesis. Clin Orthop 424:6–18, 2004.
23. Kofoed H. Scandinavian Total Ankle Replacement (STAR). Clin Orthop 424:73–79, 2004.
24. Anderson T, Montgomery F, Carlsson A. Uncemented STAR total ankle prostheses. J Bone Joint Surg Am 86(suppl 1):103–111, 2004.

E2F decoy oligodeoxynucleotide ameliorates cartilage invasion by infiltrating synovium derived from rheumatoid arthritis

TETSUYA TOMITA[1], YASUO KUNUGIZA[1,2], NARUYA TOMITA[4], HIROSHI TAKANO[1,5], RYUICHI MORISHITA[2], YASUFUMI KANEDA[3] and HIDEKI YOSHIKAWA[1]

[1]Department of Orthopaedics, [2]Divisions of Clinical Gene Therapy, [3]Gene Therapy Science, Osaka University Graduate School of Medicine, 2-2 Yamada-oka, Suita, Osaka 565-0871; [4]Division of Nephrology, Department of Internal Medicine, Kawasaki Medical School, 577 Matsushima, Kurashiki, Okayama 701-0192; [5]Second Department of Oral and Maxillofacial Surgery, Kyushu Dental College, 2-6-1 Manazuru, Kokurakita-ku, Kitakyushu 803-8580, Japan

Received January 13, 2006; Accepted March 4, 2006

Abstract. This study examined the ability of E2F decoy oligodeoxynucleotides (ODN) to inhibit proliferation of synovial fibroblasts derived from patients with rheumatoid arthritis (RA). The effect of E2F decoy ODN on cartilage invasion by RA synovium in a murine model of human RA was also investigated. E2F decoy ODN were introduced into synovial tissue and synovial fibroblasts derived from patients with RA using hemagglutinating virus of Japan (HVJ)-liposomes. The effect of E2F decoy ODN on synovial fibroblast proliferation was evaluated by MTT assay and by RT-PCR for the cell cycle regulatory genes proliferating-cell nuclear antigen (PCNA) and cyclin-dependent kinase 2 (cdk2). Changes in production of inflammatory mediators by RA synovial tissue following transfection with E2F decoy ODN were assessed by ELISA. Human cartilage and RA synovial tissue transfected with E2F decoy ODN were co-transplanted in severe combined immunodeficient (SCID) mice. After 4 weeks, the mice were sacrificed and the implants histologically examined for inhibition of cartilage damage by E2F decoy ODN. E2F decoy ODN resulted in significant inhibition of synovial fibroblast proliferation, corresponding with reduced expression of PCNA and cdk2 mRNA in synovial fibroblasts. The production of interleukin-1ß (IL-1ß), IL-6 and matrix metalloproteinase (MMP)-1 by synovial tissue was also significantly inhibited by the introduction of E2F decoy ODN. Further, in an *in vivo* model, cartilage that was co-implanted with RA synovial tissue transfected with E2F decoy ODN exhibited no invasive and progressive cartilage degradation. These data demonstrate that transfection of E2F decoy ODN prevents cartilage destruction by inhibition of synovial cell proliferation, and suggest that transfection of E2F decoy ODN may provide a useful therapeutic approach for the treatment of joint destruction in arthritis.

Correspondence to: Dr Tetsuya Tomita, Department of Orthopaedics, Osaka University Graduate School of Medicine, 2-2 Yamada-oka, Suita, Osaka 565-0871, Japan
E-mail: tomita@ort.med.osaka-u.ac.jp

Key words: decoy oligodeoxynucleotide, cartilage invasion, synovium, rheumatoid arthritis

Introduction

Rheumatoid arthritis (RA) is characterized by synovial hyperplasia with infiltration of various inflammatory cells resulting in invasion of articular cartilage and bone (1). Synovial fibroblasts are thought to play an important role in the pathogenesis of joint destruction in the arthritic joints. Synovial cells are the major source of proinflammatory cytokines and matrix metalloproteinases (MMP) such as IL-1, IL-6, TNF-α, MMP-1 and MMP-3 (2), and expression is clearly apparent at cartilage-pannus junctions (3). The importance of proliferative activity in RA and its association with production of proinflammatory cytokines has been studied (4-6). Therefore, cell cycle regulators are attractive candidates for therapeutic targets to halt joint destruction in RA.

The transcription factor E2F regulates the expression of multiple cell-cycle regulatory genes that are critical to cell growth and proliferation. In G_0/G_1 phase, E2F forms an inactive complex with the hypophoshorylated retinoblastoma (RB) gene product, cyclin A and cdk2. In this condition, the transcriptional activity sequestered E2F is repressed. Once RB is phosphorylated, E2F is released and becomes free to bind to a specific cis element in the promoter region of cell cycle regulatory genes c-myc, c-myb, cdc2, and cdk2 and proliferating cell nuclear antigen (PCNA), thereby transactivating the expression of these genes (7-10). Cell cycle biology involves a complex interaction of multiple growth factors, their receptors, secondary messengers, oncogenes and transcriptional factors. Therefore, the transcriptional factor E2F provides a good single target for cell cycle blockade.

It has been demonstrated that a synthetic double-stranded oligodeoxynucleotide (ODN) with high affinity for a target transcription factor may be introduced into target cells as a 'decoy' to bind the transcription factor, thereby altering gene transcription (11). We have previously demonstrated inhibition of synovial cell proliferation *in vitro* and amelioration

of joint damage *in vivo* using NFκB decoy ODN (12). To determine the utility of cell cycle inhibition in treating RA, the present study examined the ability of E2F decoy ODN to inhibit synovial proliferation and production of proinflammatory mediators. We also examined the effects of E2F decoy ODN on cartilage invasion by synovial tissue derived from RA patients.

Materials and methods

Patients. Synovial tissues were obtained from five patients with RA who were undergoing synovectomy at Osaka University Hospital and affiliated facilities after receipt of informed consent. All the patients were diagnosed clinically with RA according to the 1987 revised diagnostic criteria of the American College of Rheumatology (13). Normal synovial tissues were obtained from three patients who were seen for trauma and had no evidence of arthritis.

Synovial cell preparation. The synovial specimens were finely minced into small pieces, soaked in an enzyme cocktail solution containing 0.1% type IV collagenase, 0.1% hyaluronidase, and 0.01% DNase (all from Sigma Chemical Co., St. Louis, MO), and incubated for 2 h at 37°C in a shaking water bath. After removal of debris by filtration, the cells thus obtained were suspended in Dulbecco's modified Eagle's medium (DMEM), washed twice, resuspended in DMEM with 10% fetal calf serum (FCS), and seeded in culture dishes. After overnight culture, non-adherent cells were removed, while adherent cells were re-cultured. Third passage synovial cells were used in the experiments.

Cell proliferation assay. Synovial cells were seeded on to uncoated 24-well tissue culture plates (Corning Inc., Corning, NY) at 4000 cells/well. The cells were then incubated in DMEM with 10% FCS for 48 h. After transfection of decoy ODN, the medium was changed to fresh DMEM with 10% FCS. Four days after transfection, an index of cell proliferation was determined by using sulphonated tetrazolium salt, and a 4-[3-(4-iodophenyl)-2-(4-nitrophenyl)-2H-5-tetrazolio]-1,3-benzene disulphonate (WST-1) cell counting kit, which is similar to the 3-(4,5-dimethylthiazol-2-yl)-2,5-diphenyl tetrazolium bromide (MTT) assay (14). This compound produces a highly water-soluble formazan dye, which makes the assay procedure easier to perform.

Synthesis of ODN and selection of sequence targets. The sequences of phosphorothioate double-stranded ODN against the E2F-binding site and of scrambled ODN used in this study were reported previously (15). The phosphorothioate ODN utilized in this study had the following sequences:

E2F decoy ODN: 5'-CTAGATTTCCCGCG-3'
3'-TAAAGGGCGCCTAG-5'

Scramble decoy ODN: 5'-CTAGATTTCGAGCG-3'
3'-TAAAGCTCGCCTAG-5'

The E2F ODN has been shown to bind the E2F transcription factor (11,15-17). Synthetic ODN were washed in 70% ethanol, dried and dissolved in sterile Tris-ethylene diamine tetra acetic acid (EDTA) buffer (10 mM Tris, 1 mM EDTA). The supernatant was purified over a nucleic acid purification-10 (NAP-10) column (Pharmacia LKB Biotechnology, Piscataway, NJ), and the ODN concentration was quantitated by spectrophotometry. Single-strand ODNs were annealed for 2 h while gradually cooling from 80 to 25°C.

Transfection using HVJ-liposome method. Phosphatidylserine, phosphatidylcholine, and cholesterol were mixed in a weight ratio of 1:4.8:2 (12,14,18,19). The lipid mixture (10 mg) was deposited on the sides of flask by removal of tetrahydrofuran in a rotary evaporator. Dried lipid was hydrated in 200 ml of balanced salt solution (BBS; 137 mM NaCl, 5.4 mM KCl, 10 mM Tris-HCl, pH 7.6) containing synthetic double-stranded ODN. Liposomes were prepared by shaking and sonication. Purified HVJ (Z strain) was inactivated by ultraviolet irradiation (110 erg/mm²/sec) for 3 min just before use. The liposome suspension (0.5 ml, containing 10 mg of lipids) was mixed with HVJ (10,000 haemagglutinating units) in a total volume of 4 ml of BBS. The mixture was incubated at 4°C for 10 min and then for 60 min with gentle shaking at 37°C. Free HVJ was removed from the HVJ-liposomes by sucrose density gradient centrifugation. The top layer of gradient containing purified HVJ-liposomes was collected for use. Synovial tissues were cultured in a serum-free medium 6 h prior to the transfection, then washed 3 times with BBS containing 2 mM $CaCl_2$. The HVJ-liposome complex (15 mM of encapsulated ODN) was added to the synovial tissues for 30 min at 37°C. Finally, fresh medium containing 10% FCS was added to the synovial tissues, which were then incubated in a CO_2 incubator.

Estimation of the transfection efficiency. To examine the localization of the transfected FITC-labeled ODN, cryostat sections of synovium transfected with decoy ODN were prepared for fluorescence microscopy. The sections were stained with Hoechst 33342 (Sigma Chemical Co.) and observed under an ultraviolet laser scanning confocal microscope (PCM 2000; Nikon, Tokyo).

RNA extraction and RT-PCR. Twenty-four hours after transfection of E2F decoy ODN, RNA was extracted from synovial tissues by means of RNAzol (Tel-Test Inc., Friendswood, TX). Expression of PCNA, cdk2, and ß-actin mRNA were measured by RT-PCR as described previously (11). Total RNA (1 μg) prepared from synovial fibroblasts was first treated with RNAse-free DNAse. After treatment for 5 min at 94°C, the samples were subjected to reverse transcription using random hexamer primers (Perkin-Elmer Cetus, Norwalk, CT) and Molony murine leukemia virus reverse transcriptase. The primers for PCNA, cdk2, and ß-actin genes used in this study were: The PCNA 5' primer, 5'-ACTCTGCGC TCCGAAGG-3'; the PCNA 3' primer, 5'-TCTCCA ATTAGGCTAAG-3'. The cdk2 5' primer, 5'-CGCTTC ATGGAGAACTTC-3'; the cdk2 3' primer, 5'-ATGGCA GAAAGCTAGGCC-3'. The ß-actin 5' primer, 5'-TTGTAA CCAACTGGGACGATATGG-3'; the ß-actin 3' primer, 5'-GATCTTGATCTTCATGGTGCT-3'. Aliquots of RNA were amplified simultaneously by PCR (30 cycles) performed

with the step-cycle program set to denature at 94°C for 1 min, anneal at 50°C for 1 min, and extend at 72°C for 2 min. PCR products were electrophoresed on 2% agarose gels stained with ethidium bromide. We observed a linear increase in the amplification of PCR products with increased amounts of RNA up to 1 mg, as well as with increasing PCR cycle number until 30 cycles, suggesting that our results truly reflect differences in mRNA expression of PCNA and cdk2. We used ß-actin as an internal control to standardize the amount of total RNA utilized for RT-PCR. We performed other sets of RT-PCR without RNA samples as negative controls to be certain that there was no artificial amplification.

Gel mobility shift assay. The nuclear extract was prepared from cultured synovial fibroblasts using methods described previously (11,14). In brief, synovial fibroblast pellets were homogenized with a Potte-Elvehjem homogenizer in 4 volumes of ice-cold homogenization buffer [10 mM HEPES pH 7.5, 0.5 M sucrose, 0.5 mM spermidine, 0.15 mM spermin, 5 mM EDTA, 0.25 M ethylene glycol tetra acetic acid (EGTA), 7 mM ß-mercaptoethanol, 1 mM phenylmethylsulphonyl fluoride]. After centrifugation at 12,000 g for 30 min at 4°C, the pellets were lysed and homogenized in a Dounce homogenizer in 1 volume of ice-cold homogenization buffer containing 0.1% NP-40. They were then centrifuged at 12,000 g for 30 min at 4°C and the pelleted nuclei were washed twice with ice-cold buffer containing 0.35 M sucrose. The nuclei were pre-extracted with 1 volume of ice-cold homogenization buffer containing 0.05 M NaCl and 10% glycerol for 15 min at 4°C. The nuclei were then extracted with homogenization buffer containing 0.3 M NaCl and 10% glycerol for 1 h at 4°C, following which the concentration of DNA was adjusted to 1 μg/ml. After the nuclear extract was pelleted at 12,000 g for 30 min at 4°C, the supernatant was brought to 45% $(NH_4)_2SO_4$ and stirred for 30 min at 4°C. The precipitated protein was collected at 17,000 g for 30 min, resuspended in homogenization buffer containing 0.35 M of sucrose, and stored in aliquots at -70°C. E2F ODN probes were labeled at the 3' end by means of a 3' end-labeling kit (Clontech Inc., Palo Alto, CA). After end-labeling, ^{32}P-labeled ODN were purified over a nick column (Pharmacia LKB Biotechnology). Binding reactions (10 μl) including the ^{32}P-labeled probe (0.5-1 ng, 10,000-15,000 c.p.m.), and 1 μg of polydeoxy-inosinic-deoxycytidic acid (Sigma Chemical Co.) were incubated with nuclear extract for 30 min at room temperature and then loaded on to a 5% polyacrylamide gel. The gels were subjected to electrophoresis, dried, and pre-incubated with parallel samples 10 min before the addition of the labeled probe.

Enzyme-linked immunosorbent assay (ELISA) quantifications of cytokine levels in synovial tissue supernatants. After transfection of E2F decoy ODN, synovial tissues (150 mg/well) were incubated in triplicate in supplemented DMEM containing 10% FCS for 48 h at 37°C and 5% CO_2. After 48 h of incubation, the supernatants were collected and centrifuged at 600 g for 10 min and stored -20°C. The assays for human IL-1, IL-6 and MMP-1 levels in the supernatant were performed using the Quantikine human ELISA kit (R&D Systems Inc., Minneapolis, MN) by following the manufacturer's protocol.

Organ culture. The synovial tissue specimen was cut into small pieces, washed 3 times in phosphate-buffered saline (PBS), and its wet weight determined. Synovial tissues were cultured on 24-well plates at 150 mg/well in DMEM (Gibco BRL, Grand Island, NY) supplemented with 10% FCS (Hyclone Laboratories, Logan, UT). Synovial tissues were placed for 6 h prior to the transfection in a serum-free medium, then washed 3 times in BSS containing 2 mM $CaCl_2$. The HVJ-liposome complex (1000 μl) containing 1.3 mg of lipid and 50 μg of encapsulated E2F decoy ODN DNA, and HMG-1 was added to the synovial tissues. The tissues were incubated at 4°C for 5 min and then at 37°C for 30 min. After incubation the medium was changed to fresh medium containing 10% FCS.

Preparation of SCID-HuRAg mice. The previously reported SCID mouse model for human RA (20-23) was evaluated as the model for the treatment study. Six-week-old male SCID mice (CB.17/Icr; Japan Clear, Tokyo, Japan) were used for establishment of SCID-HuRAg model. Normal human articular cartilage with subchondral bone was collected from trauma patients with a femoral neck fracture after informed consent at the time of surgery. The complexes of articular cartilage 4.5-mm diameter and RA synovial tissue (100 mg) transfected with E2F decoy ODN or scramble decoy ODN were co-implanted under the skin of SCID mice. The mice were anesthetized with diethyl ether, according to the guidelines established by the Animal Ethics Committee of Osaka University Medical School. A 1-cm incision was made in the middle of the back, and paravertebral muscle was exteriorized. The back muscle was incised, and RA synovial tissue and normal human cartilage were co-implanted. The entire procedure was performed under sterile conditions.

Specimen evaluation. Forty-five days after implantation, implants were removed, immediately cut off the subchondral bone and then snap-frozen in OCT Tissue Tek. To evaluate the effect of E2F decoy ODN on cartilage invasion by RA synovial tissue, the sections were stained with hematoxylin and eosin, and invasion of the articular cartilage and degradation of perichondrocytic cartilage were evaluated by the following previously reported criteria: Invasion score: 0 = no or minimal invasion, 1 = visible invasion (~ >2 cell depths), 2 = invasion (~ >5 cell depths), 3 = deep invasion (~ >10 cell depths). Cartilage degradation scores: 0 = no degradation, 1 = visible degradation, 2 = degradation, 3 = intensive degradation (24).

Statistical analysis. Results are expressed as means ± standard error of the mean (SEM). Mann-Whitney U test was used to determine significant differences. $p<0.05$ was considered significant. All experiments were carried out at least 3 times.

Results

Transfection of FITC-labeled ODN into cells in the synovial tissue. We first verified that double-stranded ODN tagged with FITC at either the 3' or the 5' end could be introduced efficiently into synovial cell nuclei using the HVJ-liposome method. Synovial tissues were fixed 1 and 7 days after transfection and observed by fluorescence microscopy. One day after transfection without HVJ-liposome, little fluorescence was detected in synovial tissue (Fig. 1C). One day after

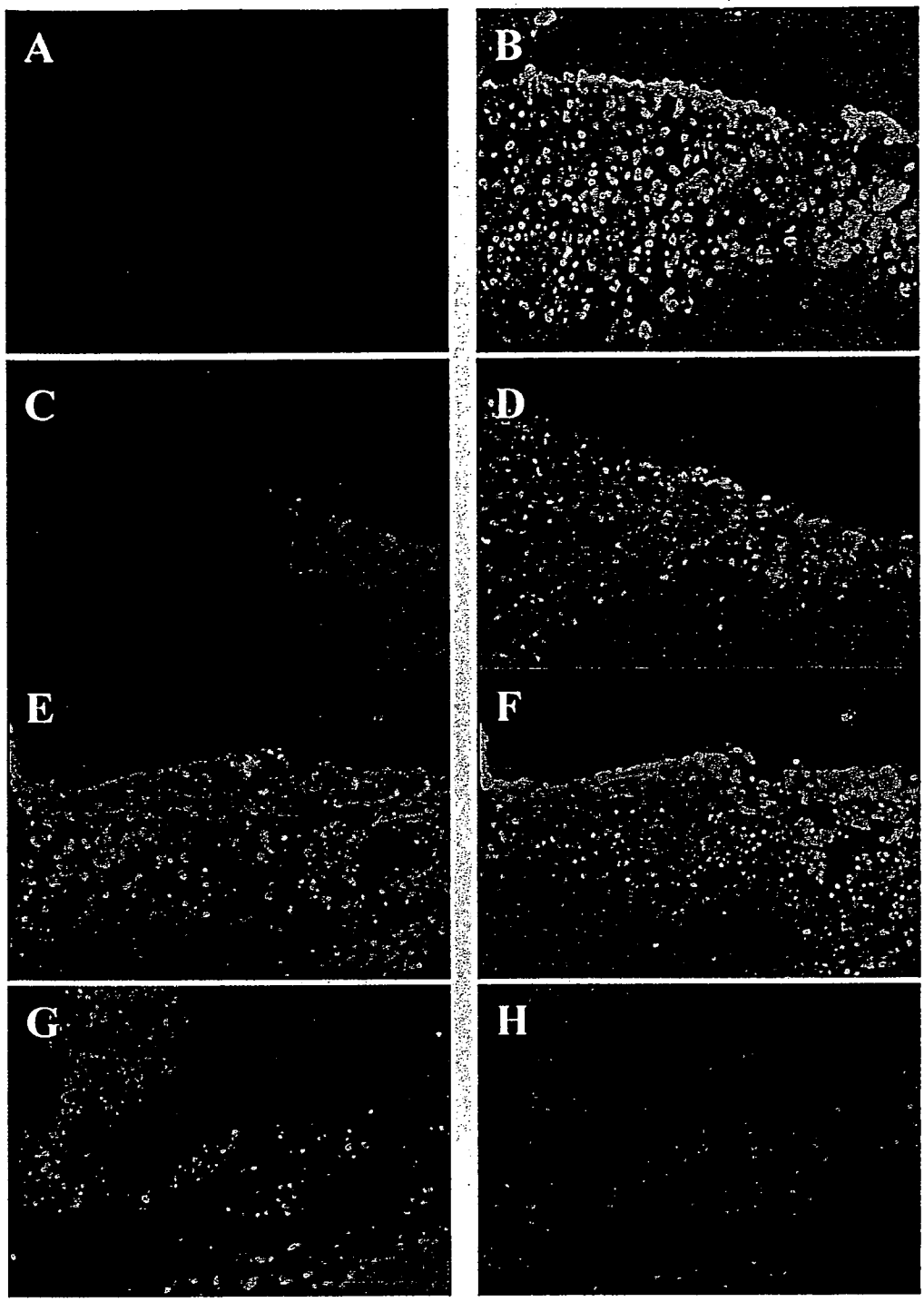

Figure 1. Uptake of FITC-labeled E2F decoy ODN into synovial tissues. Synovial tissues were transfected with FITC-labeled double-stranded ODN (1 μM) with or without the HVJ-liposome method. Synovial tissues were fixed with methanol at 1 and 7 days after transfection, and examined by fluorescence microscopy. (A) Control (transfection with HVJ-liposome method without E2F decoy ODN) (day 1, x100). (C) Direct transfection (1 μM; day 1, x100). (E) Transfection with HVJ-liposome method (1 μM; day 1, x100). (G) Transfection with HVJ-liposome method (1 μM; day 7, x100). (B, D, F and H) The section was counterstained with H&E (B, D and F; day 1, H; day 7, x100).

transfection with the HVJ-liposome method, fluorescence was detected in both the nuclei and the cytoplasm. We detected FITC-labeled ODN in the nuclei of ~50% of the cells (Fig. 1E and F). Even 7 days after transfection with HVJ-liposomes, FITC-labeled ODN were detected in both nuclei and cytoplasm (Fig. 1G and H). No fluorescent signal was seen in the non-transfected cells (Fig. 1 A).

E2F activation in synovial fibroblasts derived from RA. We examined whether or not E2F was suitable target for inhibition of proliferation of synovial fibroblasts derived from RA (Fig. 2). First, we confirmed the upregulation in E2F-binding activity in synovial fibroblasts derived from patients with RA (lane 2). When RA synovial fibroblasts were stimulated with TNF-α, an increase in E2F-binding activity was observed (lane 3). The gel mobility shift assay demonstrated that

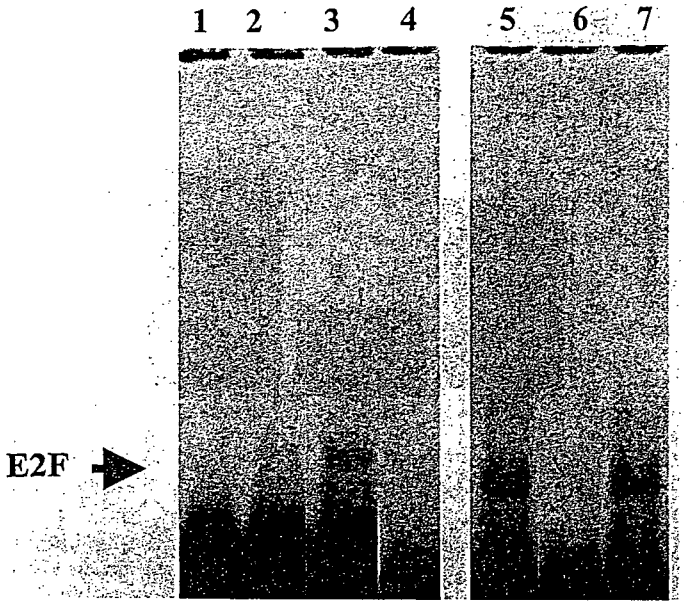

Figure 2. Gel mobility shift assay for E2F activity in nuclear extracts of synovial tissues after decoy transfection. Lane 1, no nuclear extract incubated with a ^{32}P-labeled E2F probe; lanes 2 and 3, nuclear extracts from synovial tissues with RA incubated with a ^{32}P-labeled E2F probe (lane 2, 10 μg; lane 4, 30 μg); lanes 4, nuclear extracts from normal synovial tissues incubated with a ^{32}P-labeled E2F probe (30 μg); lane 5, nuclear extracts from synovial tissues with RA transfected with HVJ-liposome solution alone; lane 6, nuclear extracts from synovial tissues with RA transfected with E2F decoy ODN (10 μM); lane 7, nuclear extracts from synovial tissues with RA transfected with scrambled decoy ODN (10 μM); Detection of E2F in nuclear extracts was specifically inhibited by E2F ODN (lane 6) but not by scrambled ODN (lane 7).

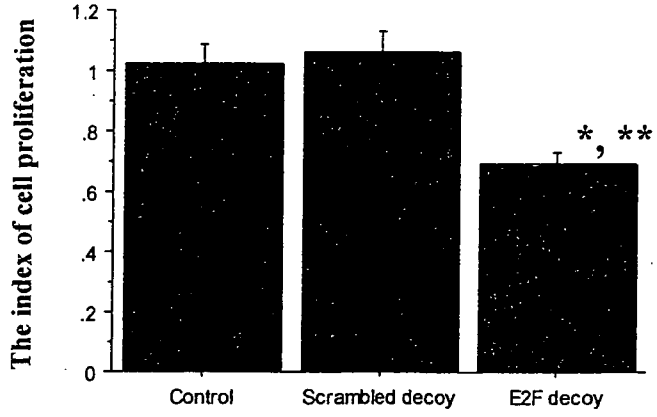

Figure 3. Inhibition of serum-stimulated synovial cells by E2F decoy ODN. The cell count assay using WST-1 was performed 4 days after transfection of decoy ODN. An index of cell proliferation was determined by absorbance at OD 450 nm. The average index of synovial fibroblast cell proliferation (n=5) was expressed as the ratio of control conditions. The result indicated reduced proliferative activity in cells transfected with E2F decoy ODN compared to the cells transfected with scrambled decoy ODN or untreated cells. Each bar represents the mean ± SE. *p<0.01 vs. non-transfected control and **p<0.01 vs. scrambled decoy ODN-treated group.

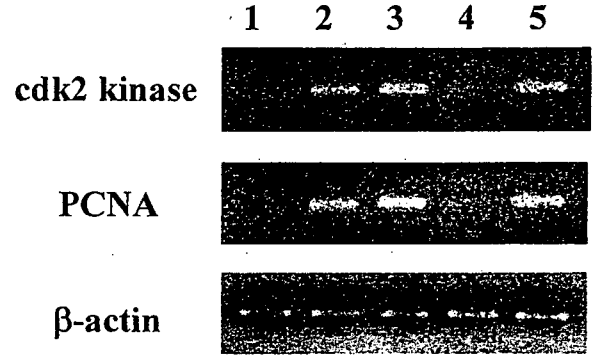

Figure 4. Changes in mRNA expression of cdk2 and PCNA by decoy transfection. Total RNA was extracted from synovial tissues 24 h after transfection with E2F decoy ODN or scrambled decoy ODN, and subjected to RT-PCR analysis for cdk2, PCNA and GAPDH. Lane 1, mRNA from synovial tissues from a trauma patient; lane 2, mRNA from synovial tissues with RA; lane 3, mRNA from synovial tissues with RA after transfection with HVJ-liposome only (without E2F decoy ODN); lane 4, mRNA from synovial tissues with RA after transfection with E2F decoy ODN using HVJ-liposome; lane 5, mRNA from synovial tissue with RA after transfection with scrambled decoy ODN. Total RNA (30 μg) was used for each blot.

E2F-binding activity was enhanced in synovial fibroblasts from patients with RA, but not in synovial fibroblasts from trauma patients (lane 4). This E2F-binding was eliminated by pre-incubation of nuclear extracts with excess amounts of unlabeled E2F ODN. Pre-incubation with excess amounts of unlabeled double-stranded scrambled ODN did not interfere with detection of E2F-binding in TNF-α stimulated synovial fibroblasts derived from RA (lanes 5-7).

Effect of E2F decoy ODN on the inhibition of synovial cell proliferation. One of the characteristic features of RA is abnormal synovial proliferation leading to joint destruction. We investigated the ability of E2F decoy ODN to inhibit synovial cell proliferation. The level of synovial cell proliferation was determined by using the WST-1 cell counting kit 4 days after transfection. The index of cell proliferation determined by absorbance at 450 nm for synovial cells transfected with E2F decoy ODN or with scrambled decoy ODN. Transfection of E2F decoy ODN resulted in a significant inhibition of synovial cell proliferation as compared with scrambled decoy ODN transfected synovial cells and non-transfected synovial cells ($p<0.01$) (Fig. 3).

Effect of E2F decoy ODN on the gene expression of synovial tissues. The transcription factor E2F plays an important role in the transactivation of the cell cycle regulatory genes. We then examined whether or not E2F inhibition would result in decrease of the downstream cell cycle genes such as PCNA and cdk2. Total RNA was extracted from synovial tissues 24 h after transfection with E2F decoy ODN or scrambled decoy ODN, and subjected to RT-PCR analysis for cdk2, PCNA and GAPDH. The expression levels of PCNA and cdk2 gene in untransfected synovial cells were upregulated. Transfection with E2F decoy ODN resulted in a marked attenuation of PCNA and cdk2 gene expression. The 18S rRNA expression level was not affected by E2F decoy ODN (Fig. 4).

Effect of E2F decoy ODN on production of inflammatory cytokines. Since proinflammatory mediators are thought to play a critical role in the pathogenesis of RA, we monitored the production of proinflammatory mediators IL-1ß, IL-6 and MMP-1. The protein levels of IL-1ß, IL-6 and MMP-1 secreted into the culture medium by RA synovial tissue were

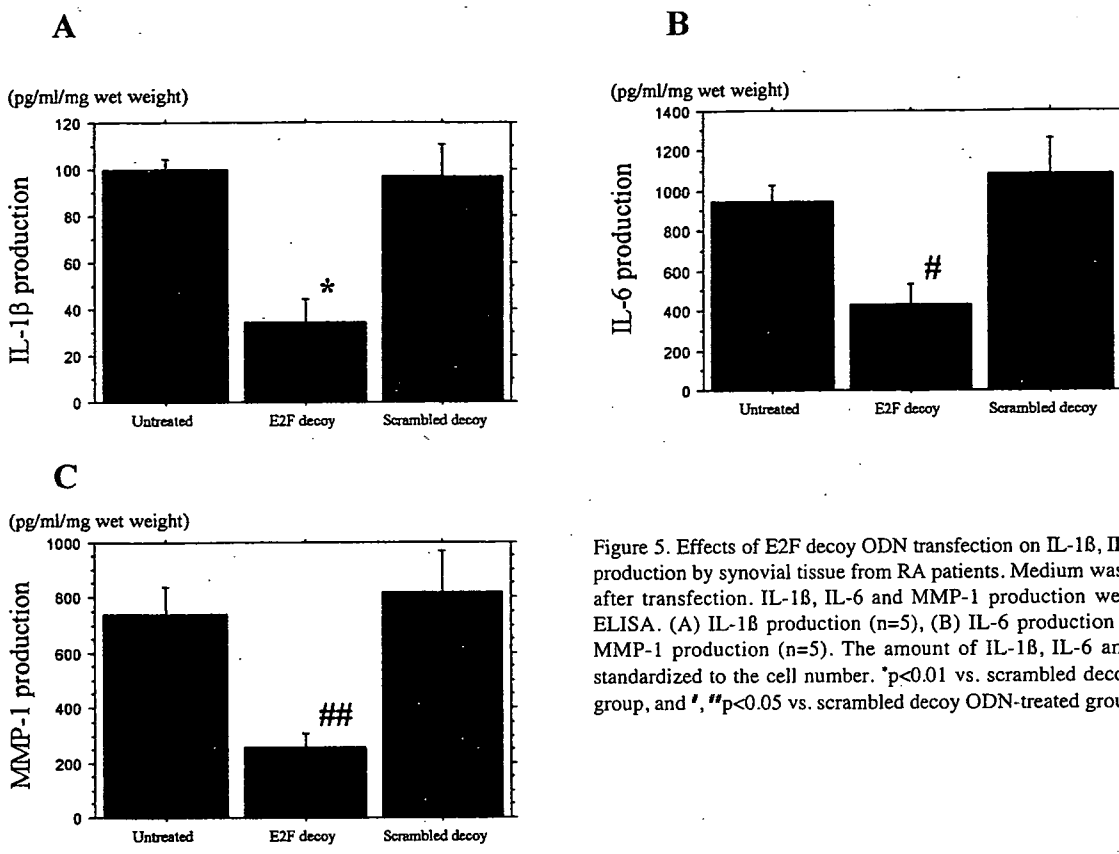

Figure 5. Effects of E2F decoy ODN transfection on IL-1ß, IL-6 and MMP-1 production by synovial tissue from RA patients. Medium was harvested 72 h after transfection. IL-1ß, IL-6 and MMP-1 production were analyzed by ELISA. (A) IL-1ß production (n=5), (B) IL-6 production (n=5) and, (C) MMP-1 production (n=5). The amount of IL-1ß, IL-6 and MMP-1 was standardized to the cell number. *p<0.01 vs. scrambled decoy ODN-treated group, and #, ##p<0.05 vs. scrambled decoy ODN-treated group.

studied 72 h after E2F decoy ODN transfection (n=5 in each group) (Fig. 5). The average level of IL-1ß was 100.2±7.2 pg/ml in untreated group and 104.7±22.5 pg/ml in scrambled decoy group, and 37.4±15.2 pg/ml in E2F decoy group, respectively. The average level of IL-6 was 995±145 pg/ml in untreated group and 1,032±120 pg/ml in scrambled decoy group, and 441±131 pg/ml in E2F decoy group, respectively. The average level of MMP-1 was 775±136 pg/ml in untreated group, 850±372 pg/ml in scrambled decoy group, and 283±76 pg/ml in E2F decoy group, respectively. E2F decoy ODN transfection reduced IL-1ß, IL-6 and MMP-1 production by 54.8±7.4, 42.4±9.5, 28.0±9.9%, respectively. Scrambled decoy ODN had no effect on the production of these mediators.

Marked suppression of invasion of cartilage by RA synovial tissue transfected with E2F decoy ODN. The therapeutic effect of E2F decoy ODN on joint destruction was examined in the severe combined immunodeficient (SCID) mice model for human RA. The volume of RA synovial tissue transfected with E2F decoy ODN was decreased as compared with untreated synovial tissue or synovial tissue transfected with scramble decoy ODN. The articular cartilage co-implanted with RA synovial tissue transfected with scramble decoy ODN showed multiple areas of synovial tissue invasion extending deep into the cartilage. The histological structure of RA synovitis was preserved in these groups. In contrast, the articular cartilage co-implanted with RA synovial tissue transfected with E2F decoy ODN showed marked suppression of invasion by synovial tissue. Infiltrating cells in synovium were decreased in this group (Fig. 6A-F). The grades of cartilage invasion co-implanted with untreated synovial tissue and synovial tissue transfected with scrambled decoy ODN ranged from 1 to 2, with an average of 1.4±0.8 and 1.8±0.4, respectively. The grades of cartilage invasion co-implanted with E2F decoy ODN transfected synovial tissue ranged from 0 to 1, with an average of 0.4±0.5. The grade of cartilage invasion was significantly lower compared with untreated or scrambled decoy ODN group (Fig. 6G).

Discussion

One of the characteristic features of RA is the extensive bone and cartilage erosion caused by the invasive proliferative synovium derived from activated fibroblasts. Thus, cell cycle modulation is an attractive therapeutic target for bone and cartilage erosion in the affected joint of RA. Recent studies demonstrated that suppression of cell cycle in synovial fibroblasts results in inhibition of experimental arthritis (25). Additionally, recent work has found that E2F functions primarily as cell proliferation, suggesting that suppression of transcription of E2F-RB complex suppresses entry into the S phase (26,27). In this study, we used transcription factor E2F decoy oligodeoxynucleotides (ODN) to inhibit synovial cell proliferation. Our data demonstrate that E2F levels in nuclear synovial fibroblast extracts were markedly increased in RA. The specificity of the radiolabeled E2F probe was confirmed by adding a 100-fold excess of unlabeled double stranded E2F decoy ODN to the reaction compared with similar quantities of missense ODN that do not bind E2F. An inhibitory effect of E2F decoy ODN on RA synovial cell proliferation *in vitro* was shown in this study, as well as in the SCID mice model for human RA. Histological examination showed marked reduction of both the volume and cellularity in synovial tissue transfected with E2F decoy ODN. We showed that nuclear E2F expression in RA synovial tissue was downregulated by transfection of E2F decoy ODN following decreased mRNA expression of the

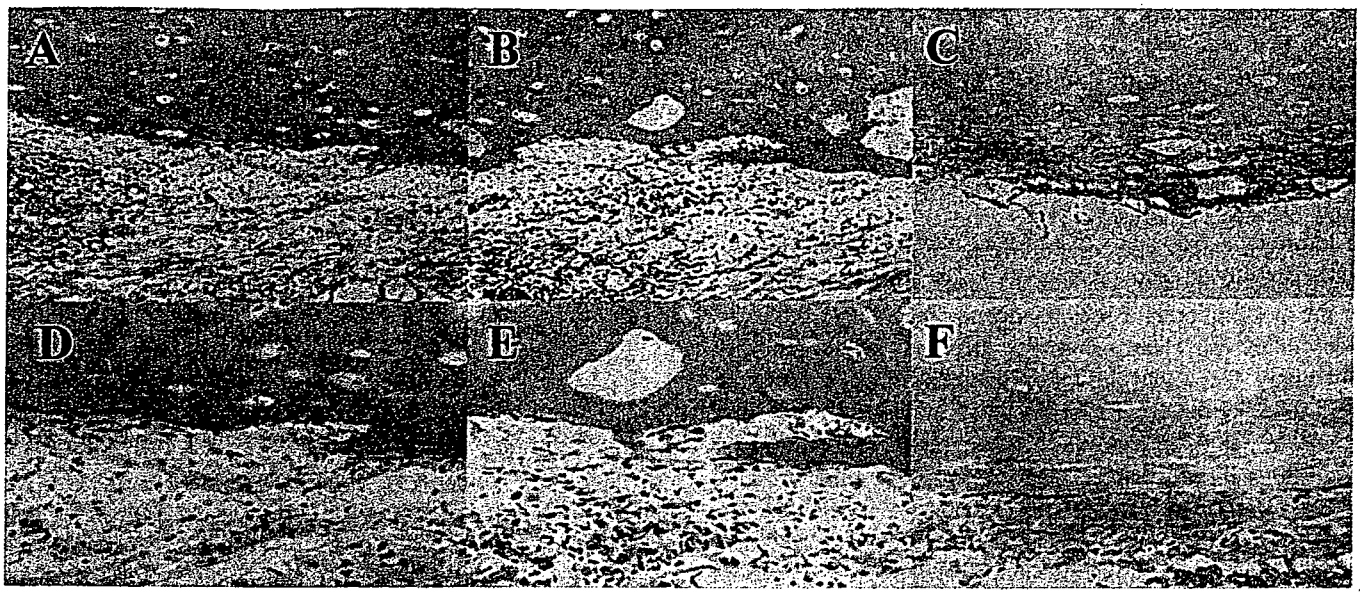

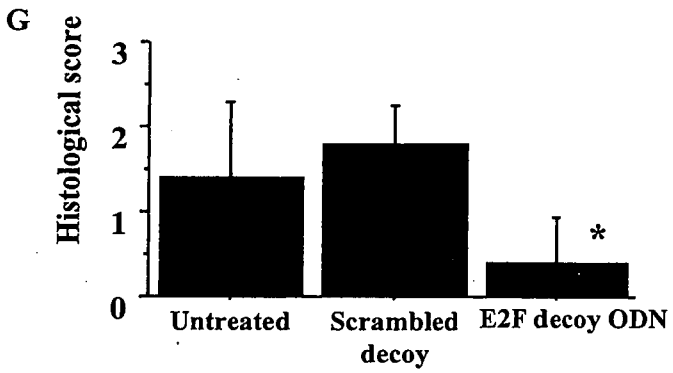

Figure 6. Histological analysis of the co-implanted synovial tissue and cartilage in SCID-HuRAg mice. (A and D) H&E stained sections from untreated synovial tissue. (B and E) H&E stained sections from synovial tissue transfected with scrambled decoy ODN. (C and F) H&E stained sections from synovial tissue transfected with E2F decoy ODN. Untreated synovial tissue and synovial tissue transfected with scrambled decoy ODN showed stratification of synovial cells and infiltration of inflammatory cells. Marked invasion of co-implanted articular cartilage by synovium is apparent (A, B, D and E). Synovial tissue transfected with E2F decoy ODN showed less hyperplasia of synovial cells and infiltration of inflammatory cells. The sections in this group mainly maintained intact cartilage (C and F). (A, B and C; original magnification x200, D, E and F; original magnification x 400). Histological score of the co-implanted synovial tissue and cartilage in SCID-HuRAg mice (n=8 in each group). There was a significant difference in histological score between E2F decoy ODN transfected group and untreated group or scrambled decoy ODN transfected group ($p<0.05$) (G).

cell cycle regulatory genes PCNA and cdk2. These results demonstrated that one mechanism by which E2F decoy ODN reduces synovial cell-associated damage is through inducing cell cycle arrest of synovial cells.

The production of proinflammatory mediators such as IL-1ß, IL-6, and MMP-1 was also suppressed by the transfection of E2F decoy ODN. This might be a secondary effect of inhibition of synovial cell proliferation, as synovial cells are the major producers of proinflammatory mediators in RA. However, the biological significance of E2F decoy ODN on proinflammatory mediator production *in vivo* still remains unclear.

One of the most important strategies for treating RA is prevention of joint destruction. We investigated the inhibitory effect of E2F decoy ODN on cartilage invasion with an *in vivo* murine model for human RA. Human normal articular cartilage and synovial tissue from patients with RA were co-implanted into SCID mice. On the basis of our *in vitro* observations, the predicted effect of E2F inhibition in this model would be prevention of cartilage invasion. The results of this study showed that transfection with E2F decoy ODN significantly suppressed cartilage invasion in this model. The exact etiology and pathogenesis have not yet been fully elucidated; however, stimulation of synovial cells by proinflammatory mediators results not only in proliferation but also in a wide variety of biological responses, including alterations in the generation of many effector molecules potentially involved in the pathological process of cartilage destruction. With respect to this point, E2F decoy ODN strategy would be beneficial not only for inducing cell cycle arrest but also for inhibition of proinflammatory mediator secretion.

New classes of technologies, such as antisense ODN, ribozymes (28-31), and RNA interference (32,33), have been adopted by the arthritis field as strategies to inhibit target gene expression in a sequence-specific manner. In the present study, we used a unique molecular strategy: a synthetic double-stranded DNA with high affinity for a target transcription factor is introduced into target cells as a decoy cis element to bind the transcription factors and alter gene transcription. We previously reported a therapeutic strategy to suppress the inflammatory process in synovial cells by transfecting decoy ODN to block the binding of the critical transcription factor NFκB to its promoter sequence of the target genes, thereby inhibiting the coordinated transactivation of genes of key cytokines and adhesion molecules necessary for the progressive joint destruction in RA (14). Joint destruction was ameliorated by the local injection of NFκB decoy ODN into the affected joints in experimental arthritis models (12). The decoy ODN strategy is more effective than antisense ODN because it blocks multiple transcriptional factors that bind to the same cis element. There are several members of the E2F family, and

this strategy of using an E2F decoy ODN inhibits all E2F members because the decoy competitively blocks binding to the cis element. This ability of decoy ODN to block all transcription factors binding to a particular cis element is the reason that we focused on this technique and we suggest that this method may be more effective than the manipulation of a single cell cycle regulatory gene.

From the therapeutic point of view, the efficiency, stability, and specificity of decoy ODN in the tissue and cellular delivery are the most important issues to address. Specificity of the E2F decoy ODN was clearly shown in this study by gel mobility shift assay. The main limitation of unmodified ODN is the rapid degradation by nucleases prevalent in sera, cell, and tissue. To rectify this problem, ODNs have been chemically modified with sulfur ions, methyl groups, or other modifications to enhance their resistance against nuclease activity. Although the stability of ODNs is enhanced by these chemical modifications, other problems have been encountered that are attributed to foreign materials (28-30). In this study, we employed a circular dumbbell structure (CD) decoy ODN instead of phosphorothioate-modified decoy ODN to overcome the disadvantages of the chemically modified form; so to enhance their uptake and stability in synovial tissue or synovial fibroblast cells, we used the phosphorothioate-modified decoy ODN and HVJ-liposome delivery system. The effectiveness and usefulness of this delivery system has been demonstrated in various disease model both *in vivo* and *in vitro* (35,36). Additional effort is now being applied to use of the circular dumbbell structure decoy ODN instead of phosphorothioate modified decoy ODN to overcome the disadvantages of the chemically modified form (37).

In conclusion, the specificity of the effects of the E2F decoy ODN is supported by the results that only transfection with E2F decoy ODN and not with scrambled decoy ODN could achieve the following effects: a) decreased E2F expression in synovial fibroblasts nuclear extracts, b) decreased mRNA expression of the cell cycle regulatory genes such as cdk2 and PCNA, c) inhibition of cell proliferation, d) decreased production of inflammatory mediators, e) amelioration of cartilage invasion. Since the induction of cell cycle progression appears to be critical for the activation of synovial cells, therapeutic strategies designed to arrest cell cycle progression may prove to be effective in treating cartilage destruction by proliferative synovitis.

Acknowledgements

We wish to thank Drs Hiroaki Matsuno and Tomoatsu Kimura for their excellent technical assistance with animal model experiments. The study was supported in part by grants from the Ministry of Education, Culture, Sport, Science and Technology of Japan, and the Ministry of Health, Labour, and Welfare of Japan.

References

1. Firestein GS: Invasive fibroblast-like synoviocytes in rheumatoid arthritis. Passive responders or transformed aggressors? Arthritis Rheum 39: 1781-1790, 1996.
2. Farahat MN, Yanni G, Poston R and Panayi GS: Cytokine expression in synovial membranes of patients with rheumatoid arthritis and osteoarthritis. Ann Rheum Dis 52: 870-875, 1993.
3. Chu CQ, Field M, Allard S, Abney E, Feldmann M and Maini RN: Detection of cytokines at the cartilage/pannus junction in patients with rheumatoid arthritis: implications for the role of cytokines in cartilage destruction and repair. Br J Rheumatol 31: 653-661, 1992.
4. Michael VV and Alisa KE: Cell cycle implications in the pathogenesis of rheumatoid arthritis. Front Biosci 5: D594-D601, 2000.
5. Nasu K, Kohsaka H, Nonomura Y, Terada Y, Ito H, Hirokawa K and Miyasaka N: Adenoviral transfer of cyclin-dependent kinase inhibitor genes suppresses collagen-induced arthritis in mice. J Immunol 165: 7246-7252, 2000.
6. Perlman H, Bradley K, Liu H, Cole S, Shamiyeh E, Smith RC, Walsh K, Fiore S, Koch AE, Firestein GS, Haines GK 3rd and Pope RM: IL-6 and matrix metalloproteinase-1 are regulated by the cyclin-dependent kinase inhibitor p21 in synovial fibroblasts. J Immunol 170: 838-845, 2003.
7. Dalton S: Cell cycle regulation of the human cdc2 gene. EMBO J 11: 1797-1804, 1992.
8. Thalmeier K, Synovzik H, Mertz R, Winnacker EL and Lipp M: Nuclear factor E2F mediates basic transcription and transactivation by E1a of the human MYC promoter. Genes Dev 3: 527-536, 1989.
9. Wagner S and Green MR: Retinoblastoma. A transcriptional tryst. Nature 352: 189-190, 1991.
10. Watson RJ, Dyson PJ and McMahon J: Multiple c-myb transcript cap sites are variously utilized in cells of mouse haemopoietic origin. EMBO J 6: 1643-1651, 1987.
11. Morishita R, Gibbons GH, Horiuchi M, Ellison KE, Nakama M, Zhang L, *et al*: A gene therapy strategy using a transcription factor decoy of the E2F binding site inhibits smooth muscle proliferation *in vivo*. Proc Natl Acad Sci USA 92: 5855-5859, 1995.
12. Tomita T, Takeuchi E, Tomita N, Morishita R, Kaneko M, Yamamoto K, *et al*: Suppressed severity of collagen-induced arthritis by *in vivo* transfection of nuclear factor kappaB decoy oligodeoxynucleotides as a gene therapy. Arthritis Rheum 42: 2532-2542, 1999.
13. Arnett FC, Edworthy SM, Bloch DA, McShane DJ, Fries JF, Cooper NS, *et al*: The American Rheumatism Association 1987 revised criteria for the classification of rheumatoid arthritis. Arthritis Rheum 31: 315-324, 1988.
14. Tomita T, Takano H, Tomita N, Morishita R, Kaneko M, *et al*: Transcription factor decoy for NFkappaB inhibits cytokine and adhesion molecule expressions in synovial cells derived from rheumatoid arthritis. Rheumatology 39: 749-757, 2000.
15. Tomita N, Horiuchi M, Tomita S, Gibbons GH, Kim JY, Baran D, *et al*: An oligonucleotide decoy for transcription factor E2F inhibits mesangial cell proliferation *in vitro*. Am J Physiol 275: F278-F284, 1998.
16. Mann MJ, Whittemore AD, Donaldson MC, Belkin M, Conte MS, Polak JF, *et al*: *Ex vivo* gene therapy of human vascular bypass grafts with E2F decoy: the PREVENT single-centre, randomised, controlled trial. Lancet 354: 1493-1498, 1999.
17. Ehsan A, Mann MJ, Dell'Acqua G and Dzau VJ: Long-term stabilization of vein graft wall architecture and prolonged resistance to experimental atherosclerosis after E2F decoy oligonucleotide gene therapy. J Thorac Cardiovasc Surg 121: 714-722, 2001.
18. Morishita R, Sugimoto T, Aoki M, Kida I, Moriguchi A, Tomita N, *et al*: *In vivo* transfection of cis element 'decoy' against nuclear factor-kappaB binding site prevents myocardial infarction. Nat Med 3: 894-899, 1997.
19. Kaneda Y, Saeki Y and Morishita R: Gene therapy using HVJ-liposomes: the best of both worlds? Mol Med Today 5: 298-303, 1999.
20. Geiler T, Kriegsmann J, Keyszer GM, Gay RE and Gay S: A new model for rheumatoid arthritis generated by engraftment of rheumatoid synovial tissue and normal human cartilage into SCID mice. Arthritis Rheum 37: 1664-1671, 1994.
21. Müller-Ladner U, Kriegsmann J, Franklin BN, Matsumoto S, Geiler T, Gay RE and Gay S: Synovial fibroblasts of patients with rheumatoid arthritis attach to and invade normal human cartilage when engrafted into SCID mice. Am J Pathol 149: 1607-1615, 1996.
22. Matsuno H, Sawai T, Nezuka T, Uzuki M, Nishimoto N, Tsuji H, and Yoshizaki K: Treatment of rheumatoid synovitis with anti-reshaping human interleukin-6 receptor monoclonal antibody: use of rheumatoid arthritis tissue implants in the SCID mouse model. Arthritis Rheum 41: 2014-2021, 1998.

23. Matsuno H, Yudoh K, Katayama R, Nakazawa F, Uzuki M, Sawai T, Yonezawa T, Saeki Y, Panayi GS, Pitzalis C and Kimura T: The role of TNF-alpha in the pathogenesis of inflammation and joint destruction in rheumatoid arthritis (RA): a study using a human RA/SCID mouse chimera. Rheumatology 41: 329-337, 2002.
24. Müller-Ladner U, Evans CH, Franklin BN, Roberts CR, Gay RE, Robbins PD and Gay S: Gene transfer of cytokine inhibitors into human synovial fibroblasts in the SCID mouse model. Arthritis Rheum 42: 490-497, 1999.
25. Taniguchi K, Kohsaka H, Inoue N, Terada Y, Ito H, Hirokawa K, *et al*: Induction of the p16INK4a senescence gene as a new therapeutic strategy for the treatment of rheumatoid arthritis. Nat Med 5: 760-767, 1999.
26. Murga M, Fernandez-Capetillo O, Field SJ, Borlado LR, Moreno B, Fujiwara Y, *et al*: Mutation of E2F2 in mice causes enhanced T lymphocyte proliferation, leading to the development of autoimmunity. Immunity 15: 959-970, 2001.
27. Harbour JW and Dean DC: Rb function in cell-cycle regulation and apoptosis. Nat Cell Biol 2: E65-E67, 2000.
28. Flory CM, Pavco PA, Jarvis TC, Lesch ME, Wincott FE, Beigelman L, Hunt SW 3rd and Schrier DJ: Nuclease-resistant ribozymes decrease stromelysin mRNA levels in rabbit synovium following exogenous delivery to the knee joint. Proc Natl Acad Sci USA 93: 754-758, 1996.
29. Jarvis TC, Bouhana KS, Lesch ME, Brown SA, Parry TJ, Schrier DJ, Hunt SW 3rd, Pavco PA and Flory CM: Ribozymes as tools for therapeutic target validation in arthritis. J Immunol 165: 493-498, 2000.
30. Takahashi M, Funato T, Suzuki Y, Fujii H, Ishii KK, Kaku M and Sasaki T: Chemically modified ribozyme targeting TNF-alpha mRNA regulates TNF-alpha and IL-6 synthesis in synovial fibroblasts of patients with rheumatoid arthritis. J Clin Immunol 22: 228-236, 2002.
31. Rutkauskaite E, Zacharias W, Schedel J, Muller-Ladner U, Mawrin C, Seemayer CA, Alexander D, Gay RE, Aicher WK, Michel BA, Gay S and Pap T: Ribozymes that inhibit the production of matrix metalloproteinase 1 reduce the invasiveness of rheumatoid arthritis synovial fibroblasts. Arthritis Rheum 50: 1448-1456, 2004.
32. Schedel J, Seemayer CA, Pap T, Neidhart M, Kuchen S, Michel BA, Gay RE, Muller-Ladner U, Gay S and Zacharias W: Targeting cathepsin L (CL) by specific ribozymes decreases CL protein synthesis and cartilage destruction in rheumatoid arthritis. Gene Ther 11: 1040-1047, 2004.
33. Zwicky R, Muntener K, Goldring MB and Baici A: Cathepsin B expression and down-regulation by gene silencing and antisense DNA in human chondrocytes. Biochem J 367: 209-217, 2002.
34. Zhou HW, Lou SQ and Zhang K: Recovery of function in osteoarthritic chondrocytes induced by p16INK4a-specific siRNA *in vitro*. Rheumatology 43: 555-568, 2004.
35. Kaneda Y, Yamamoto S and Hiraoka K: The hemagglutinating virus of Japan-liposome method for gene delivery. Methods Enzymol 373: 482-493, 2003.
36. Kaneda Y, Uchida T, Kim J, Ishiura M and Okada Y: The improved efficient method for introducing macromolecules into cells using HVJ (Sendai virus) liposomes with gangliosides. Exp Cell Res 173: 56-69, 1987.
37. Tomita N, Tomita T, Yuyama K, Tougan T, Tajima T, Ogihara T and Morishita R: Development of novel decoy oligonucleotides: advantages of circular dumb-bell decoy. Curr Opin Mol Ther 5: 107-112, 2003.

疾患と骨質

②関節リウマチ

Bone quality in rheumatoid arthritis

柏井　将文・橋本　　淳・吉川　秀樹

Masafumi Kashii, Jun Hashimoto(助教授), *Hideki Yoshikawa*(教授)／大阪大学大学院医学系研究科医学部器官制御外科(整形外科)

関節リウマチ(RA)は続発性骨粗鬆症の原因の一つであり，RAに続発する骨粗鬆症は傍関節性骨粗鬆症と全身性骨粗鬆症に分けられる．ステロイド非使用のRA患者に続発する骨粗鬆症は高回転型の骨代謝動態を示すことが多い．現在，臨床的に骨強度を評価し得るパラメーターとしては骨密度，骨代謝マーカーを用いた骨代謝回転評価，マクロレベルでの構造特性があるが，それ以外の臨床的に骨強度評価の不可能なパラメーターは骨質という概念でまとめられている．近年になり，RA続発の骨粗鬆症での骨質変化についての検討がいくつか報告されるようになってきたが，今後のさらなる検討が待たれる．

key words

関節リウマチ
全身性骨粗鬆症
傍関節性骨粗鬆症
骨密度
骨代謝回転

はじめに

関節リウマチ(RA)は，傍関節性骨粗鬆症(juxtaarticular osteoporosis)や全身性骨粗鬆症(generalized osteoporosis)といった続発性骨粗鬆症の原因疾患であることが知られており，脆弱性骨折が多いために骨質低下の存在が指摘されている[1)-3)]．2000年のNIH(National Institute of Health)コンセンサス会議にて，「骨粗鬆症は骨強度の低下によって骨折のリスクが増大する骨疾患であり，骨強度は骨密度と骨質の両者を反映する」と定義され，その内容は2001年のJAMA誌に掲載された[4)]．それ以降，骨質が新しいパラダイムとして注目され，さまざまな議論を呼んでいる．

骨強度は構造特性(ジオメトリー，微細構造)と材料特性(ミネラル・コラーゲン・マイクロダメージ)により決定されるものであり，これらの諸特性は骨代謝(骨モデリング・骨リモデリング)によって制御されている．現在，臨床的に骨強度を評価し得るパラメーターとしては，骨密度，骨代謝マーカーを用いた骨代謝回転評価，マクロレベルでの構造特性があるが，それ以外の臨床的に骨強度評価の不可能なパラメーターは骨質という概念でまとめられ，その中で重要な位置にあるのがミクロレベルでの構造特性と材料特性である(表1)．

近年，骨微細構造評価や石灰化度・コラーゲン架橋の解析など，RAに続発する骨粗鬆症の骨質評価が進められている．ステロイド性骨粗鬆症と骨質との関連については他稿に譲ることとし，本稿においてはステロイド非使用のRAに合併する骨粗鬆症の研究から得られた骨質に関する知見について記載する．

骨代謝動態と関節リウマチ

炎症関節局所にみられる傍関節性骨粗鬆症はX線写真上早期に認められる変化であり，滑膜組織などより産生される炎症性サイトカイン(IL-1，IL-6，TNF-αなど)や閉経による骨吸収亢進，局所の不動による骨形成低下が関与している[3)5)]．一方，全身性骨粗鬆症は多因子が関与し，より複雑な骨代謝動態を示す．炎症性サイトカ

表1　骨強度の規定因子

1. 骨　量
2. 骨　質
①構造特性
・マクロレベル：サイズ，形状，皮質骨幅
・ミクロレベル：海綿骨梁の微細構造，皮質骨多孔性
②材料特性
・無機成分：総石灰量，石灰化度，結晶サイズ
・有機成分：コラーゲンタイプ，コラーゲン架橋状況(成熟度)
・マクロダメージ，マイクロクラック
・材料異方性：コラーゲン/ミネラル配向度

骨強度は骨量と骨質より構成され，骨質は構造特性と材料特性に大別される．しかしながら，これらの諸特性だけでは骨強度を説明するには不十分であり，材料組織化・異方化の概念の導入が必要である．

イン，閉経，各種ホルモン異常などが骨吸収亢進に関与し，ステロイド投与，不動などが骨形成低下に関与している[3)5)]．ステロイド非使用のRA患者の大半が閉経後骨粗鬆症同様に高回転型骨代謝動態を示す[6)]．骨吸収マーカーに関しては，尿中デオキシピリジノリン，尿中NTxの増加が活動期RAにて認められるとの報告が多く，血中IL-6，CRP値，RA活動性と骨吸収マーカーが相関すると報告されている[7)]．したがって，RAでは骨代謝動態の高回転化により，骨密度減少，吸収窩拡大，骨微細構造の劣化が引き起こされ骨強度の低下をきたす．

骨質と関節リウマチ

RAに合併する骨粗鬆症とその骨質に関する検討はこれまであまり行われていなかったが，近年徐々に検討されつつある．RAにおける骨質の研究について，以下に紹介する．

1. 骨の構造特性

マイクロCTの開発が進み，三次元的に骨梁微細構造を定量的に解析することが可能となり，骨折抑制効果への骨微細構造変化の寄与の重要性が認識されるようになってきた．海面骨梁の数・幅・連結性などは力学的応力に適応した構造を示し，骨強度に対して大きく寄与している．Garcia-Miguelらは，ステロイド非使用のRA患者14例と年齢・性別を合わせたコントロール群14例より腸骨を採取し，マイクロCTにて解析を行った[8)]．その結果，RA群では有意な海綿骨量の低下，骨梁幅の低下，骨梁連結性の低下が認められ，RA群の海綿骨微細構造が低下していることが明らかになった．

2. 骨の材質特性

1)ミネラル

骨基質内の石灰化量・石灰化度・結晶サイズなどが骨強度に関与する．高代謝回転状態の骨では，新しい骨単位の形成が多いため，石灰化度が低いことが知られている．しかし，骨基質内の石灰化度の不均一性は高い．骨基質内の石灰化度の分布幅は広すぎても狭すぎても骨強度が低下する．石灰化度が高いほど骨硬度は高まるが，同時に石灰化度が均一化すると，あるレベル以降"硬いが脆い骨"となり骨強度は低下する[9)]．

斎藤らは，RA患者12例および年齢・性別を合わせたコントロール群10例より大腿骨頚部骨を採取し，石灰化度分布およびカルシウム(Ca)，リン(P)含有量についての検討を行った[10)]．その結果，RA群ではコントロール群に比べて，低石灰化度骨の含有量が高く，低・高石灰化度分画のCa，P含有量は海綿骨では低下した．RA群の海綿骨では，高骨代謝回転動態を反映した結果，二次石灰化度が低下していることが明らかになった．

2)コラーゲン

材料学的には，骨は繊維強化型複合材料に分類される．二つ以上の異なる特性をもつ素材を複合化することにより，それぞれのもつ素材の欠点が補われ，それらよりも優れたあるいは全く新しい機能を発揮させることが可能である．繊維状の材料は，強度の寸法効果*により極めて高い強度を発現させることが可能である．繊維の集合体は引張荷重に対しては非常に強いが，単なる集合体では圧迫荷重，捻りモーメン

＊：細くなると材料的強度が増加する．材料はサイズが小さくなるほど強度が増す．

ト，曲げモーメントに対しては抵抗できない．そのため，最も高い強度を生み出す繊維状の材料を構造材料として用いるには，マトリックスとの複合化が必須となる．骨の場合，コラーゲン線維が「繊維状の材料」に相当し，その質(コラーゲン架橋量，架橋種類)・量が骨強度に関与する．

斎藤らは，前述のRA群とコントロール群にて，ミネラルの検討に加えコラーゲン量，コラーゲン架橋量(生理的架橋，非酵素的糖化架橋)についても検討を行った[10]．架橋分析の結果，生理的架橋については皮質骨・海綿骨での成熟架橋量に差が認められなかったのに対し，未熟架橋はRA群で低下していた．さらに，RA群では非酵素的糖化架橋(advanced glycation end products：AGEs)が増加し，コラーゲン脆弱指数が増加した．TNF-αが生理的架橋形成を阻害することや，AGEsが酸化ストレスで誘導されることが知られており，これらの知見より局所のサイトカインがコラーゲンの質を悪化させる可能性があることが示唆される．

関節リウマチの骨粗鬆症に対する治療

RA患者における骨質を規定する諸因子に関する検討についていくつか紹介したが，現時点では，臨床上骨質を直接評価し得るパラメーターはなく，骨代謝マーカーを用いた骨代謝回転動態評価が行われている．

1. 関節リウマチのコントロール

RAの活動性を制御することにより，傍関節性骨粗鬆症を予防し治療することが可能である．また，RAに合併する全身性骨粗鬆症患者では，不動などで身体活動性が低下することにより，主に大腿骨頚部や踵骨など荷重部で骨量減少が進行することが知られている．そのため，全身性骨粗鬆症の予防・治療に際しては，身体活動性の保持・改善が重要であり，適切な運動療法や関節リウマチ治療薬による治療が必要となる．

現在，最も広く使用されているメトトレキサート(MTX)の投与により，骨吸収マーカーが低下し，RAの活動性を制御することにより骨粗鬆症が予防されることが示されている[11)12)]．インフリキシマブのようなTNF-αを直接阻害する薬剤も，RAの活動性を制御することにより骨吸収マーカーを低下させ，大腿骨頚部や腰椎の骨密度を増加させることが示されており，RA患者における骨粗鬆症の予防・治療が期待できる[13)-15)]．また，ヒト化抗IL-6レセプター抗体(トシリズマブ)についても，近年その骨代謝動態に対する効果が報告されている[16)17)]．西本らは，トシリズマブ4mg/kgあるいは8mg/kgの4週間に1回投与を52週間行った群において，骨形成マーカーであるPICP，オステオカルシンの有意な上昇と骨吸収マーカーである尿中デオキシピリジノリンの有意な低下を認めたことを報告している(表2)．さらに橋本らは，トシリズマブ8mg/kgの4週間に1回投与を52週間行った群ではMTXを中心とした既存治療群に比較して腰椎・大腿骨頚部の骨密度の低下が有意に抑制されることを明らかにした．トシリズマブは既存治療群に比して骨粗鬆症進行を予防し，この効果はステロイド減量，歩行能力改善，RAの活動性の抑制，のいずれの関与も推測される．骨質を規定する諸因子が骨リモデリング・骨モデリングにより制御されていることから考えると，関節リウマチ治療薬により骨代謝動態を改善させることで，骨質が改善・保持される可能性がある．

2. 骨吸収治療薬

現在，原発性骨粗鬆症に対して明らかな骨折抑制効果のエビデンスをもつ薬剤として，ビスフォスフォネート製剤，選択的エストロゲン受容体モジュレーターがある．高骨代謝回転動態を示す骨粗鬆症に対し骨吸収抑制剤を投与すれば，劣化した骨微細構造が改善し骨基質骨石灰化度が上昇する[18)]．また，骨吸収抑制剤投与によるこれらの骨質を規定する諸因子を改善することにより，骨強度が上昇することが知られている．

RAに続発する全身性骨粗鬆症に対するビスフォスフォネート投与の有効性について多くの報告がなされている[19)20)]．しかしながら，報告のほとんどはステロイド投与を受けている患者を含めているため，純粋にステロイドフリーのRA患者における全身性骨粗鬆症へのビスフォスフォネート投与の効果については完全に立証されているわけではない．なお，ステロイドフリー

表2　ヒト化抗IL-6レセプター抗体(トシリズマブ)の骨代謝動態に対する効果

	プラセボ (n＝54)	4mg/kg (n＝54)	8mg/kg (n＝55)
オステオカルシン (ng/mL)			
ベースライン	5.8±2.8	5.7±2.8	5.1±2.2
12週間投与後	6.2±3.1	6.6±3.1*	6.5±2.7*
PICP (ng/mL)			
ベースライン	135.4±65.7	127.0±63.5	117.2±47.7
12週間投与後	144.3±77.8	146.4±70.6*	166.4±78.7*
尿中ピリジノリン (μmol/mol Cr)			
ベースライン	60.3±32.6	58.8±32.7	58.5±29.8
12週間投与後	62.6±30.9	49.0±29.5*	47.4±24.2*
尿中デオキシピリジノリン (μmol/mol Cr)			
ベースライン	7.8±3.4	7.6±3.5	7.4±3.1
12週間投与後	7.6±3.8	6.6±3.2*	6.9±3.1*

*：$p<0.05$ vs. 各項目ベースライン値(t検定)，平均値±標準偏差で表示．
PICP：I型プロコラーゲン-C-プロペプチド

(文献16)より一部改変して掲載)

のRAモデル動物においては，骨吸収マーカーの低下および骨微細構造の保持が認められ，ビスフォスフォネートの有効性が示されている[21)22)]．また，ビスフォスフォネート投与は実験上RAの炎症抑制効果を示し，さらに傍関節性骨粗鬆症への有効性が動物実験で示されている[21)-23)]．しかしながら，RA患者の傍関節性骨粗鬆症に対するビスフォスフォネート投与の効果についての報告は少なく，またその規模も小さいことから，RA患者におけるRAの炎症抑制効果や傍関節性骨粗鬆症への有効性に関して結論を出すまでにはいまだ検討を必要とする．

おわりに

関節リウマチ，特にステロイド非使用の関節リウマチ患者に合併する骨粗鬆症と骨質に関して概説した．骨質の概念そのものがクローズアップされるようになって間もないためか，RAに合併する骨粗鬆症とその骨質に関する検討は少ない．RA患者における骨質の変化について，関節リウマチ治療薬や骨吸収抑制剤の骨質への効果についての今後の検討が待たれる．

また，骨質そのものについても完全に全貌がつかまれているわけではない．骨はマクロレベルからナノレベルまで精緻に制御された複合材料であり，積層化や繊維強化などさまざまな組織化形態を取ることで，加えられた応力に対して最適な材料を構築している[24)]．力学的応力に適応するべく皮質骨・海綿骨を異方化させるメカニズムについてはほとんどわかっていないが，材料異方性は骨強度に対して極めて強い影響を与えることが知られている[25)26)]．身近な例で例えれば，鉄筋コンクリート材は内部の鉄筋の走行方向の違いに

よりその力学特性は大きく異なることと同様である．現在，骨質は構造特性と材料特性に大きく二別されているが，これらの特性だけでは骨強度を説明するには不十分であり，材料組織化・異方化の観点からの骨質に対するアプローチも必要である．

文 献

1) Gough AKS, Lilley J, Eyre S, et al : Generalized bone loss in patients with early rheumatoid arthritis. Lancet **344** : 23-27, 1994
2) Dequeker J, Maenaut K, Verwilghen J, et al : Osteoporosis in rheumatoid arthritis ; a review. Clin Exp Rheumatol **13** (Suppl.12) : S21-26, 1995
3) Sambrook PN : The skeleton in rheumatoid arthritis ; common mechanisms for bone erosion and osteoporosis? J Rheumatol **27** : 2541-2542, 2000
4) NIH Consensus Development Panel : Osteoporosis prevention, diagnosis, and therapy. JAMA **285** : 785-795, 2001
5) Deodhar AA, Woolf AD : Bone mass measurement and bone metabolism in rheumatoid arthritis ; a review. Br J Rheumatol **35** : 309-322, 1996
6) al-Awadhi AM, Olusi SO, al-Zaid NS, et al : Urine levels of type 1 collagen cross-linked N-telopeptides and deoxypyridinoline correlate with disease activity in rheumatoid arthritis. Clin Exp Rheumatol **16** : 569-572, 1998
7) Gough A, Sambrook P, Devlin J, et al : Osteoclastic activation is the principal mechanism leading to secondary osteoporosis in rheumatoid arthritis. J Rheumatol **25** : 1282-1289, 1998
8) Garcia-Miguel J, Wright AC, Perez-Edo L, et al : Bone microarchitecture changes in rheumatoid arthritis assessed by 3D micro-CT. 28th annual meeting of the ASBMR abstracts : S109 F-327, 2006
9) Boivin G, Meunier PJ : Methodological considerations in measurement of bone mineral content. Osteoporos Int **14** (Suppl.5) : 22-28, 2003
10) 斎藤 充，田中孝昭，曽雌 茂：関節リウマチ患者における骨質因子としての骨石灰化度とコラーゲン架橋形成．第23回日本骨代謝学会学術集会プログラム抄録：167 O-25, 2005
11) Gough AK, Peel NF, Eastell R, et al : Excretion of pyridinium crosslinks correlates with disease activity and appendicular bone loss in early rheumatoid arthritis. Ann Rheum Dis **53** : 14-17, 1994
12) Kollerup G, Hansen M, Horslev-Petersen K : Urinary hydroxypyridinium cross-links of collagen in rheumatoid arthritis. Relation to disease activity and effects of methylprednisolone. Br J Rheumatol **33** : 816-820, 1994
13) Ostanek L, Pawlik A, Brzosko I, et al : The urinary excretion of pyridinoline and deoxypyridinoline during rheumatoid arthritis therapy with infliximab. Clin Rheumatol **23** : 214-217, 2004
14) Lange U, Teichmann J, Muller-Ladner U, et al : Increase in bone mineral density of patients with rheumatoid arthritis treated with anti-TNF-α antibody ; a prospective open-label pilot study. Rheumatol **44** : 1546-1548, 2005
15) Torikai E, Kageyama Y, Takahashi M, et al : The effect of infliximab on bone metabolism markers in patients with rheumatoid arthritis. Rheumatol **45** : 761-764, 2006
16) Nishimoto N, Yoshizaki K, Miyasaka N, et al : Treatment of rheumatoid arthritis with humanized anti-interleukin 6 receptor antibody. Arthritis Rheum **50** : 1761-1769, 2004
17) 橋本 淳，宮坂信之，山本一彦，他：ヒト化抗IL-6レセプター抗体(トシリズマブ)治療は関節リウマチ患者にみられる骨粗鬆症進行を防止する．第24回日本骨代謝学会学術集会プログラム抄録：188 O-96, 2006
18) Boivin GY, Chavassieux PM, Santora AC, et al : Alendronate increases bone strength by increasing the mean degree of mineralization of bone tissue in osteoporotic

柏井 将文(Masafumi Kashii)
1976年 和歌山県生まれ
2000年 大阪大学医学部医学科卒業
2000～2004年 大阪大学医学部付属病院・信州大学医学部付属病院・市立豊中病院に勤務
2004年～ 大阪大学大学院医学系研究科器官制御外科(整形外科)